

Supporting Information

Title: Monitoring Assembly of Virus Capsids with Nanofluidic Devices

Authors: Zachary D. Harms, Lisa Selzer, Adam Zlotnick, and Stephen C. Jacobson

Materials. We purchased sodium chloride from Mallinckrodt; 4-(2-hydroxyethyl)-1-piperazineethanesulfonic acid (HEPES) and methanol from Sigma-Aldrich Co.; ammonium hydroxide from J.T. Baker; hydrogen peroxide from Macron Fine Chemicals; sodium hydroxide from Fisher Scientific; Microposit MF-319 developer from Rohm and Haas Electronic materials; chromium etchants 8002-A and 1020 and buffered oxide etchant from Transene Co., Inc.; D263 glass substrates with a 120-nm thick layer of chromium and a 530-nm thick layer of photoresist from Telic Co.; #1.5 cover slip glass from VWR, Inc.; Anotop 10 syringe filters from Whatman GmbH; and 353NDT Epoxy from Epoxy Technology, Inc.

Preparation and Purification of Cp149 Dimer. The Cp149 dimer samples were prepared as follows. The Cp149 gene encoding core protein monomer was expressed in *E. coli* with a pET11-based vector. The cell solution was lysed by sonication, and cell debris was removed by centrifugation for 1 h at 200,000 g. Cp149 dimers were then purified by size exclusion chromatography (SEC) between multiple steps of assembly and disassembly. Cp149 capsids obtained from the cell lysate were purified by SEC over a 1 L Sepharose® CL-4B column equilibrated in 100 mM HEPES pH 7.5, 100 mM NaCl, 2 mM DTT. Capsids were disassembled by adding solid urea to a final concentration of 3 M for 1.5 h at 4 °C, and the resulting dimers were purified by SEC over a 1.5 L Sephacryl® S-300 column equilibrated in Buffer N (50 mM NaHCO₃ pH 9.6 + 2 mM DTT at 4 °C). To separate assembly active dimer from inactive dimer, an additional assembly step was initiated by adding 5 M NaCl to a final concentration of 0.3 M NaCl for 2 h at room temperature. Assembled capsids were then purified again by SEC over a

1.5 L Sephacryl® S-300 column equilibrated in Buffer N. Capsids were disassembled by adding solid urea to a final concentration of 3 M for 1.5 h at 4 °C, and dimers were purified by SEC over a 1.5 L Sephacryl® S-300 equilibrated in Buffer N. All capsid and dimer fractions were concentrated to 2 mg/ml after each purification step with a stirred cell pressure concentrator (EMD Millipore). For each experiment, an aliquot of frozen Cp149 dimer was thawed and dialyzed into 50 mM HEPES pH 7.5 prior to use. Each dimer aliquot was subjected to only one freeze and thaw cycle, and after purified dimer aliquots were thawed, formation of T = 3 or T = 4 capsids is not detectable by TEM and SEC analysis.¹

Calibration of Nanofluidic Devices. Before each assembly experiment, the nanofluidic devices were calibrated with purified T = 3 and T = 4 capsid standards. Calibration allows unambiguous assignment of the T = 3 and T = 4 distributions in the histograms of the assembly products. **Figure S1** shows three example histograms of $\Delta i/i$ for T = 3 capsids, T = 4 capsids, and a 1:1 mixture of T = 3 to T = 4 capsids. For the data in **Figure S1**, T = 3 capsids displace $0.43\% \pm 0.2\%$ of baseline current, and T = 4 capsids displace $0.62\% \pm 0.3\%$. The heights of the T = 3 and T = 4 distributions are nearly equal at 0.1 counts/total, indicating that the nanopores are not biased towards sensing the smaller T = 3 capsids. However, the T = 3 distribution has a width of 0.042%, whereas the T = 4 distribution has a width of 0.056%. The T = 4 distribution is systematically wider than the T = 3 distribution in the assembly experiments.

Calibration of Capsid Concentration. The counts/min in the resistive-pulse data are directly proportional to the concentration of analyte. In **Figure S2**, a purified 100 nM T = 4 capsid standard was used to make a series of dilutions, and each solution was tested on the same device with an applied potential of 500 mV. The nanopores do not preferentially sense T = 3 capsids over T = 4 capsids. Solution molarity is converted to particles/mL to generate a

calibration curve with a slope of 2.49×10^{-10} mL·counts/particles/min, a y-intercept of -9.5 counts/min, and an R^2 of 1.0.

Assembly near the Pseudo-Critical Dimer Concentration. **Figure S3** shows a histogram of $\Delta i/i$ for the assembly products formed from 0.9 μM Cp149 dimer in 1 M NaCl over a 60 min reaction. $T = 3$ and $T = 4$ capsids are the primary particles present and displace 0.58% and 0.83% of the baseline current ($\Delta i/i$), respectively. Intermediates are present with notable $\Delta i/i$ distributions at 0.71% (105 dimers) and 0.47% (77 dimers). However, almost all of these intermediates are recorded in the first few minutes of the assembly reaction. Overall, assembly of 0.9 μM dimer in 1 M NaCl produces 74% $T = 4$ capsids and 20% $T = 3$ capsids.

Transmission Electron Microscopy. The fractions of $T = 3$ capsids, $T = 4$ capsids, and intermediates formed in the assembly reactions are verified by transmission electron microscopy (TEM). At various time points during assembly, the reaction is quenched by depositing a 2.5 μL aliquot of the reaction mixture onto a copper TEM grid. The grid is then stained with uranyl acetate. The same samples are tested by both TEM and resistive-pulse sensing, and the TEM results compare favorably with resistive-pulse measurements for all reactions analyzed.

TEM images are taken of particles formed from 5, 7, and 10 μM Cp149 dimer assembled in 1 M NaCl after 15 s and 24 h of reaction. **Figure S4** shows a TEM image of the particles from 10 μM dimer after 15 s of reaction. $T = 3$ capsids, $T = 4$ capsids, and a number of intermediates are observed. TEM results are compared to resistive-pulse data in **Table S1**, where the fractions of $T = 3$ capsids, $T = 4$ capsids, and intermediates are determined by each method. Intermediates are the particles with sizes between the $T = 3$ and $T = 4$ capsids. From 15 s to 24 h, the fraction of $T = 3$ capsids is constant, the fraction of $T = 4$ capsids increases, and the fraction of intermediates decreases. Agreement between resistive-pulse and TEM data is excellent and improves as dimer

concentration increases, because the number particles that can be counted in the TEM images increases.

Elongation Rate. Growth of T = 3 and T = 4 capsids is monitored over time. In **Figure S5a**, the fraction of T = 4 capsid formed is plotted over time for dimer concentrations ranging from 50 nM to 0.9 μ M. Each growth curve is fitted to the function:

$$(S1) \quad y = \frac{Ax}{B+x}$$

where A is the equilibrium percentage of capsid formed, and B is the time for the reaction to reach 50% completion, referred to as the lag time. In **Figure S5b**, lag time is plotted as a function of the inverse of the initial dimer concentration and is proportional to the elongation rate for the formation of capsids. For T = 4 capsids, the elongation rate constant (f) is calculated from the slope of the fitted line (m) in **Figure S5b** by:

$$(S2) \quad f = \frac{117}{m}$$

where the constant of 117 is the number of steps in the elongation reaction for a T = 4 capsid, assuming a nucleation size of three dimers.^{2,3} An elongation rate constant is calculated to be $1.71 \times 10^7 \text{ M}^{-1}\text{s}^{-1}$ and is comparable to reported values for HBV assembly.⁴

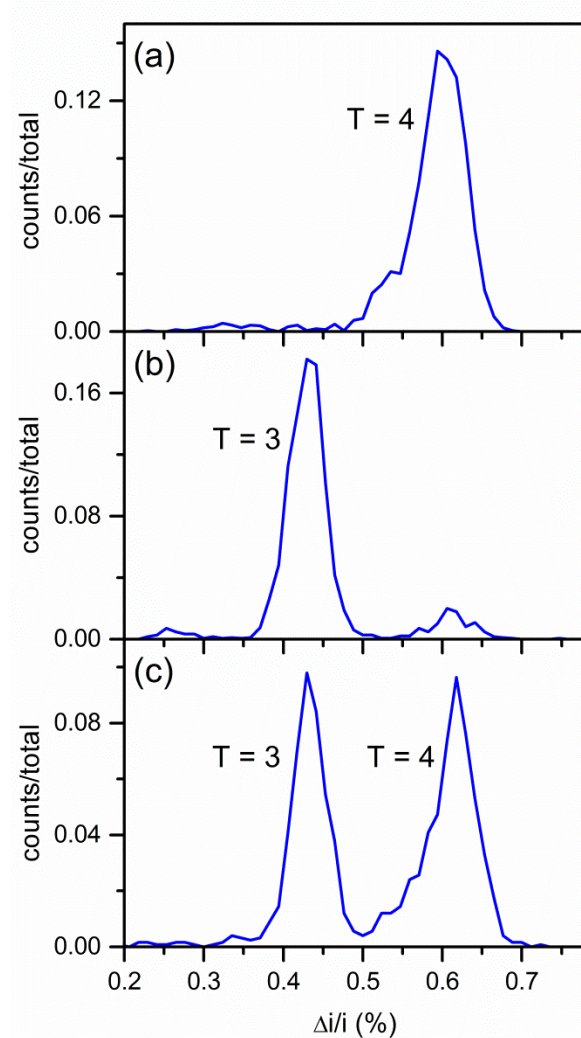


Figure S1. Histograms of $\Delta i/i$ for T = 3 and T = 4 capsid standards. Pulse amplitude is divided by baseline current to obtain $\Delta i/i$ for (a) purified T = 4 capsids, (b) purified T = 3 capsids, and (c) a 1:1 mixture of T = 3 and T = 4 capsids.

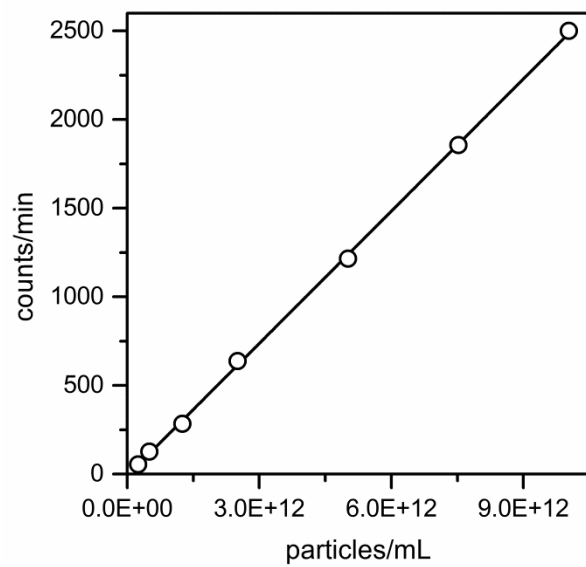


Figure S2. Variation of counts/min with capsid concentration for resistive-pulse sensing. Linear fit to the data has a slope of 2.49×10^{-10} and an R^2 of 1.0.

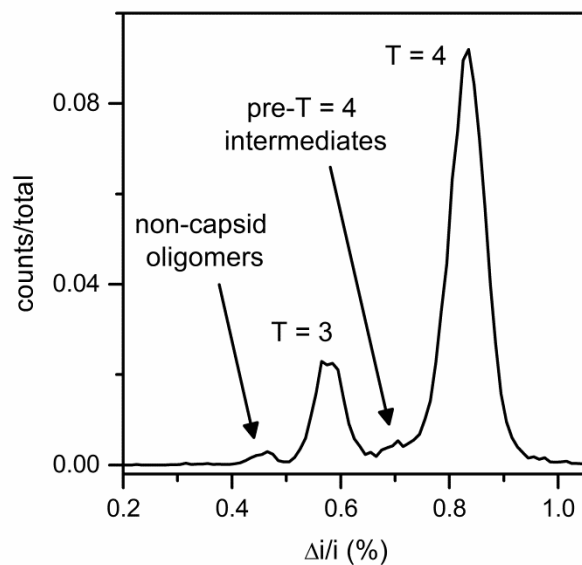


Figure S3. Histogram of $\Delta i/i$ for an assembly reaction at 0.9 μM Cp149 dimer in 1 M NaCl. Assembly products over a 60 min reaction show distributions corresponding to T = 3 capsids, T = 4 capsids, non-capsid oligomers, and pre-T = 4 intermediates are present. Total counts are > 14,000 particles.

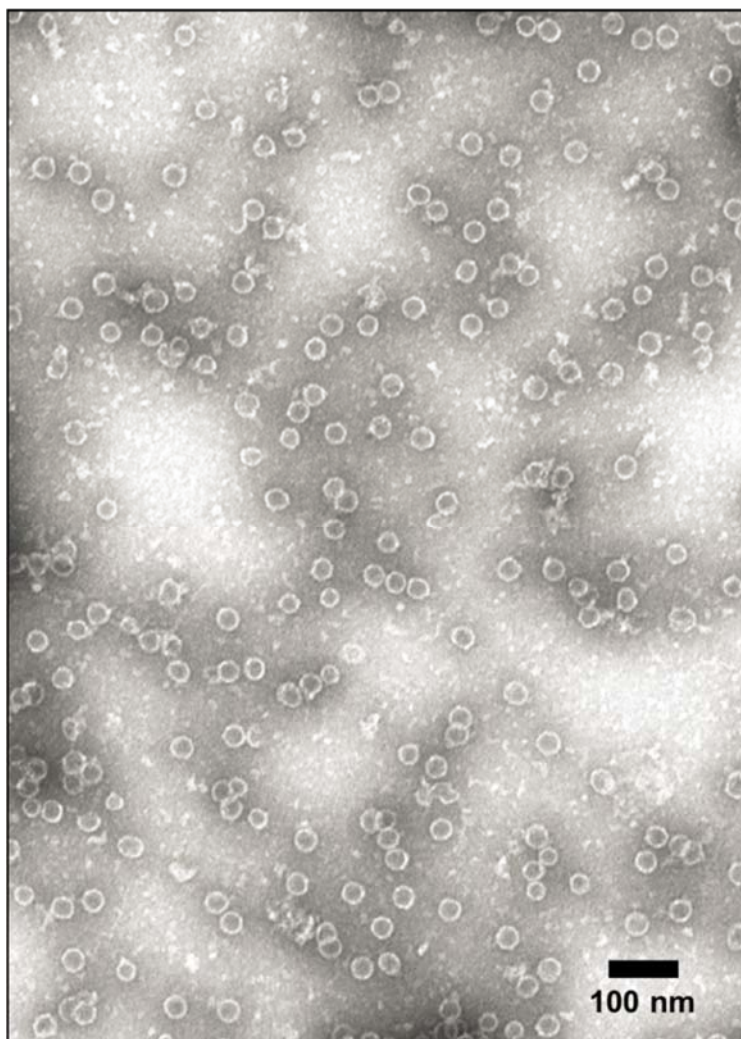


Figure S4. Transmission electron microscope (TEM) image of capsids assembled from 10 μ M Cp149 dimer in 1 M NaCl after 15 s of reaction. In addition to T = 3 and T = 4 capsids, intermediates are observed that have sizes smaller than the T = 3 capsids and between the T = 3 and T = 4 capsids.

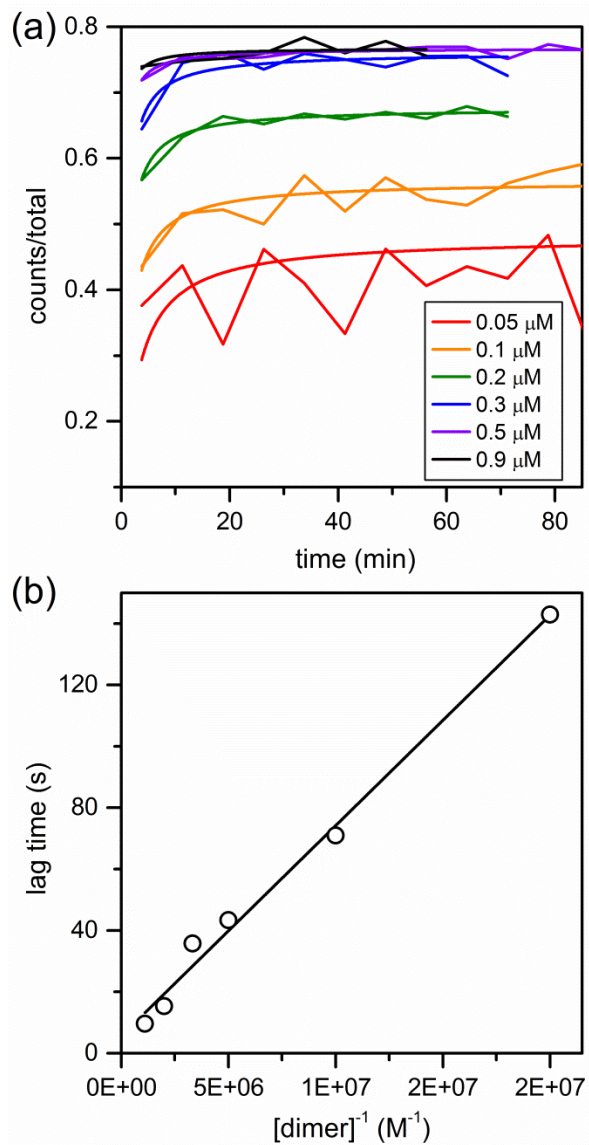


Figure S5. (a) Growth curves of T = 4 capsids for dimer concentrations from 0.05 to 0.9 μM . Data are fitted with Equation S1 to determine the lag time, at which the reaction is 50% complete. (b) Variation of lag time with inverse dimer concentration for T = 4 capsids. The slope of the fitted line is proportional to the elongation constant of $1.71 \times 10^7 \text{ M}^{-1}\text{s}^{-1}$. Total counts are > 1300, 5000, 10,000, 8000, 17,000, and 48,000 for 0.05, 0.1, 0.2, 0.3, 0.5, and 0.9 μM dimer, respectively.

	10 μ M, 15 s		10 μ M, 24 h	
	Nanopore	TEM	Nanopore	TEM
% T = 4	64.9	66.2	76.3	73.1
% Intermediate	13.5	12.4	4.8	10.4
% T = 3	18.4	21.4	16.2	16.6

	7 μ M, 15 s		7 μ M, 24 h	
	Nanopore	TEM	Nanopore	TEM
% T = 4	60.9	55.4	75.9	73.5
% Intermediate	13.2	25.9	5.0	8.25
% T = 3	19.1	17.4	17.1	18.3

	5 μ M, 15 s		5 μ M, 24 h	
	Nanopore	TEM	Nanopore	TEM
% T = 4	63.6	37.3	76.7	55.8
% Intermediate	14.5	34.2	4.8	12.8
% T = 3	20.0	28.5	16.6	31.3

Table S1. Comparison of resistive-pulse sensing data to transmission electron microscopy (TEM) images (see **Figure S4**). T = 3 capsids, T = 4 capsids, and intermediates with sizes between T = 3 and T = 4 capsids are counted after 15 s and 24 h of reaction by both techniques. Total counts from TEM images are 266, 527, and 1,073 for 5, 7, and 10 μ M dimer, respectively. Total counts for resistive-pulse sensing are > 40,000, 29,000, and 29,000 for 5, 7, and 10 μ M dimer, respectively.

References

- (1) Tan, Z.; Maguire, M. L.; Loeb, D. D.; Zlotnick, A. Genetically Altering the Thermodynamics and Kinetics of Hepatitis B Virus Capsid Assembly Has Profound Effects on Virus Replication in Cell Culture. *J. Virol.* **2013**, *87*, 3208-3216.
- (2) Zlotnick, A.; Johnson, J. M.; Wingfield, P. W.; Stahl, S. J.; Endres, D. A Theoretical Model Successfully Identifies Features of Hepatitis B Virus Capsid Assembly. *Biochemistry* **1999**, *38*, 14644-14652.
- (3) Hagan, M. F.; Elrad, O. M. Understanding the Concentration Dependence of Viral Capsid Assembly Kinetics-the Origin of the Lag Time and Identifying the Critical Nucleus Size. *Biophys. J.* **2010**, *98*, 1065-1074.
- (4) Selzer, L.; Katen, S. P.; Zlotnick, A. The Hepatitis B Virus Core Protein Intradimer Interface Modulates Capsid Assembly and Stability. *Biochemistry* **2014**, *53*, 5496-5504.